Heliyon 10 (2024) e37273

Contents lists available at ScienceDirect

Heliyon

journal homepage: www.cell.com/heliyon

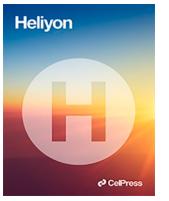

Research article

Flavonoid glycosides from *Odontonema strictum* leaves

Jean Claude W. Ouédraogo [a,*], Céline Henoumont [b], Irène Semay [c], Félix B. Kini [d], Sophie Laurent [b], Pascal Gerbaux [c], Yvonne L. Bonzi – Coulibaly [a]

[a] *Laboratoire de Chimie Analytique, Environnementale et Bio-Organique (LCAEBiO), Université Joseph KI-ZERBO, 03 BP 7021, Ouagadougou 03, Burkina Faso*

[b] *General, Organic and Biomedical Chemistry Unit, Nuclear Magnetic Resonance (NMR) and Molecular Imaging Laboratory, University of Mons - UMONS, 23 Place du Parc, B-7000, Mons, Belgium*

[c] *Organic Synthesis and Mass Spectrometry Laboratory, Interdisciplinary Center for Mass Spectrometry, Research Institute for Biosciences, University of Mons - UMONS, 23 Place du Parc, B-7000, Mons, Belgium*

[d] *Département Médecine-Pharmacopée Traditionnelles et Pharmacie, Institut de Recherche en Sciences de la Santé (IRSS), CNRST, 03 BP 7192, Ouagadougou 03, Burkina Faso*

ARTICLE INFO

Keywords:
Odontonema strictum (Acanthaceae)
Flavonoids
LC–MS
NMR

ABSTRACT

Odontonema strictum (Acanthaceae) leave extract was investigated for its flavonoid content. Column chromatography was used for compound isolation and mass spectrometry was performed using electrospray ionization (ESI) in the negative ion mode for compound identification.

The full characterization of luteolin 7-*O*-[β-D-apiofuranosyl-(1 → 2)-*O*-β-D-ribofuranoside], a flavone glycoside, was achieved using tandem mass spectrometry and high resolution 1D and 2D Nuclear Magnetic Resonance (NMR). Among the 10 flavonoids glycosides detected in the ethanol extract, beside the isolated one, 3 flavone glycosides with luteolin or apigenin aglycone were tentatively identified.

1. Introduction

The plant species *Odontonema strictum* of the Acanthaceae family is commonly used in Burkina Faso to fight against hypertension. This plant is nowadays more and more envisaged for a large range of biomedical and pharmaceutical applications, due to the broad spectrum of reported biological activities, including antihypertension [1,2], antibacterial [3] and antioxidant [4] properties. Phytochemical screenings revealed the presence of phytoconstituents belonging to many families, including tannins, flavonoids, steroids, saponins, carbohydrates and glycosides [3]. A mixture of well-known phytosterols (stigmasterol and β-sitosterol) was isolated, characterized [5] and showed antibacterial activity [6]. Several phenylpropanoid glycosides (verbascoside and isoverbascoside) were isolated from *Odontonema strictum* leaves and exhibited potent radical scavenging activities against DPPH and H_2O_2 free radicals [7]. The antioxidant capacity of *Odontonema strictum* leaves extracts correlates quite well with the measured total phenolic and total flavonoid contents, indicating the important contribution of phenolic compounds to the antioxidant properties [4]. In previous studies, flavonoids have been identified as the major group of specific metabolites in *Odontonema strictum* leaves [4,8], but no molecule has been isolated and fully characterized up to date. The literature mentioned the isolation of a flavonoid, proposed to be tiliroside, but its structure was not firmly established [9]. In a previous report on the identification of *Odontonema strictum* metabolites, three flavonoids have been detected but the glycosylation sites and bindings were not fully elucidated [4]. Besides being an integral component of the

* Corresponding author.
E-mail address: ouedraclaude@yahoo.fr (J.C.W. Ouédraogo).

https://doi.org/10.1016/j.heliyon.2024.e37273
Received 22 April 2023; Received in revised form 22 August 2024; Accepted 30 August 2024
Available online 30 August 2024

human diet with medicinal value, flavonoids also present biopesticide potentialities [10,11] and show good activity against micro-organisms [12], cereal fungi [13] and termites [14]. Therefore, the isolation and identification of the flavonoids extracted from *Odontonema strictum* leaves become mandatory from a structure/activity relationship point of view, but also to permit their (semi-) industrial applications since the control and quality regulations enforced in industrial environments now require complete knowledge of the molecules present in the formulations.

In the present study, we reinvestigated the flavonoid content of the *Odontonema strictum* ethanol extract. We successfully *(i)* isolated and identified the most abundant flavonoid, and *(ii)* performed a thorough qualitative and quantitative analysis of the major flavonoid glycosides. Several analytical methods have been employed to achieve our objectives, including column separation, Liquid Chromatography-Mass Spectrometry (LC-MS), tandem MS (MS/MS) analysis, and ^{1}H and ^{13}C Nuclear Magnetic Resonance (NMR) spectroscopy.

2. Material and methods

2.1. General experimental procedures

Extraction, column chromatography and Thin Layer Chromatography (TLC) were performed using ethanol, methanol, chloroform, butanol, ethyl acetate and formic acid purchased from Sigma-Aldrich. Column chromatography was performed with silica gel (230–400 mesh) (Sigma-Aldrich). Gel permeation chromatography was performed on Sephadex LH-20 from Pharmacia (Uppsala, Sweden) and Diaion HP-20 reverse phase column from Supelco. TLC was performed on silica gel 60 F_{254} plates (Merck, Darmstadt, Germany).

Standards, namely luteolin, apigenin, diosmin, kaempferol-7-*O*-neohesperidoside were purchased from Sigma-Aldrich (Paris-France).

The LC-MS analyses were performed with methanol, acetonitrile and acetic acid HPLC grade, purchased from Merck (Darmstadt, Germany). Milli-Q water was prepared using a Veolia Pure Lab flex 2 generator (Veolia, Brussels, Belgium).

2.2. Plant material and extraction

The leaves of *Odontonema strictum* were collected from the garden of the Department of Traditional Medicine, Institute for Health Sciences Research at Ouagadougou (Burkina Faso). The collected plant material was compared to a previous voucher specimen (N°8702) deposited in the Herbarium of the National Centre for Scientific and Technological Research (Ouagadougou, Burkina Faso). The leaves were shade dried, powdered and stored in an air tight container till further use. One and half kilogram (1.50 kg) of leaves powder was first defatted with cyclohexane and then extracted with 15 L ethanol 70 % by stirring the mixture at room temperature for 24 h. The EtOH extract was filtered, centrifuged (Centriguge OSI, Italy) for 10 min at 2000 g and then concentrated on a rotavapor under reduced pressure to give 72.42 g of a dried ethanol extract (4.83 % w/w).

2.3. Isolation and purification

Ethanol extract (72 g) was subjected to Diaion HP-20 column (MeOH–H_2O, 3 × 50 cm), in order to remove the chlorophyll and waxes, by increasing the gradient of methanol in water [15]. Twelve fractions were collected and analyzed by TLC with Neu reagent as a derivatizing reagent. The fractions containing the main flavonoid were gathered and submitted to separation on silica gel column (230–400 mesh, 3 × 40 cm) using $CHCl_3$–MeOH gradient (0–100%MeOH). TLC was used to follow the separation during the column chromatography. Forty fractions were collected and based on TLC profile, those containing the targeted spot were subjected to repeated Sephadex LH-20 column chromatography (MeOH, 2.2 × 154 cm) to yield the compound **1** (25 mg), as an amorphous powder with orange color.

2.4. NMR spectra analysis

The NMR spectra of the isolated flavonoid (**1**) were recorded at 298 K in Dimethyl sulfoxide-d_6 (DMSO-d_6) on a Bruker Ascend 600 spectrometer operating at 14.09 T (600 MHz for ^{1}H and 150.90 MHz for ^{13}C). The chemical shift scales were calibrated using the signal of the solvent (2.50 ppm for ^{1}H and 39.50 ppm for ^{13}C) or the signal of internal TMS (0.00 ppm). 2 D NMR spectra were recorded as described in the literature [16].

2.5. LC–MS/MS analysis

The LC device used consisted of a Waters Alliance 2695, coupled to a Micromass Q-ToF Ultima API-US (Manchester UK) type mass spectrometer, equipped with an electrospray source. The column used at a temperature of 40 °C was Phenomenex Kinetex C18, 150 × 2.1 mm, 5 μm. The mobile phase, at a flow rate of 0.25 mL/min, consisted of a mixture of milli-Q water (0.01 % HCOOH) (eluent A) and methanol (eluent B) according to the gradient 10 % of B for 0–6 min, 30 % of B for 6–11 min, 35 % of B for 11–18 min, 50 % of B for 18–23 min, 90 % of B for 23–25 min, 100 % of B for 25–27 min and at the end 10 % B for 27–30 min. The sample (1 mg/mL in methanol) was injected at a volume of 10 μL.

The parameters used for the MS analyses in negative mode were: capillary voltage 3.1 kV, cone voltage 40 V, source temperature

100 °C, desolvation temperature 120 °C, desolvation gas - dry N_2 (500 L/h). The electrospray negative ionization mode (ES $^-$) were used. The mass spectra in full scan mode were recorded by means of the Time-of-Flight (ToF) type analyser operating at a resolution of 8000 over a mass range *m/z* 50–2000. For LC–MS/MS analyses, selected ions were collided against argon in the six-pole collision cell at sufficient collision energy to induce a rate of sufficient decomposition.

The exact masses were determined using diosmin and kaempferol-7-*O*-neohesperidoside as internal standards.

2.6. Estimation of the relative abondance of flavonoids

In order to describe most of the flavonoids in the ethanol extract, we used a previously described methods [17,18] to estimate the relative abundance of each flavonoid within the ethanol extract. This estimation was achieved using the extracted LC–MS signal integration for each flavonoid molecular ion. The integration of the LC–MS signals allowed estimating the proportion of each flavonoid in the extract. The relative abondance, the aglycone type, the glycosides composition and the retention time of each flavonoid was generated using Microsoft Excel 2019.

3. Results and discussion

3.1. Flavonoid profiling in the ethanol extract

Ethanol is commonly used for flavonoid extraction from the biomass [19]. After drying and weighing, the leaves of *Odontonema strictum* were defatted with cyclohexane and extracted with ethanol 70 % at room temperature for 24 h under stirring. The filtered ethanol extract was subjected to Diaion HP-20 column separation. A rough phytochemical screening was realized all along the elution from the column by thin layer chromatography (TLC) using the Neu reagent to detect flavonoids. The fractions containing flavonoids were pooled and evaporated to dryness under reduced pressure. The dried extract was reconditioned in methanol for liquid chromatography - mass spectrometry (LC-MS) analysis as described in the literature [20]. The obtained chromatogram is shown in Fig. 1.

The total ion current (TIC) chromatogram of the ethanol extract features seven major signals (Fig. 1) that are ascribed to flavonoid derivatives based on the TLC analysis, with measured *m/z* at 579.1, 549.1, 563.1, 533.1, 591.1, 577.1 and 605.1 for, respectively, the signals detected at 15.77, 16.59, 18.04, 18.54, 18.94, 20.25 and 21.01 min (Fig. 1). A closer analysis allows detecting additional flavonoids at 16.61 min and 18.19 min that are observed as *m/z* 547.1 and *m/z* 593.1 ions respectively, leading to a total of 9 different compositions. Extracted Ion Current (EIC) chromatograms (Figure S1.1-9), are further built to detect isomers. Roughly, a dominant isomer is detected for all the compositions, except for the *m/z* 563 ions that appear at a 35:65 ratio at two different elution times, 18.04 and 18.93 min. Minor isomers are detected for the *m/z* 547 and 591 ions. In a first quantitative analysis, we reported in Table 1 the relative abundances of all the detected flavonoid ions (by merging the minor isomers for *m/z* 547 and 591). The two isomers detected at *m/z* 563 are distinguished in Table 1 due to their high abundances. Globally, 10 different molecules are constituting the flavonoid extract of the leaves of *Odontonema strictum*.

3.2. Flavonoid isolation

The ethanol extract was further fractionated on silica gel column using $CHCl_3$–MeOH gradient to isolate the dominant flavonoids for further analysis, typically by targeting compound **1** in Table 1. Forty fractions were collected and based on TLC screening (Neu

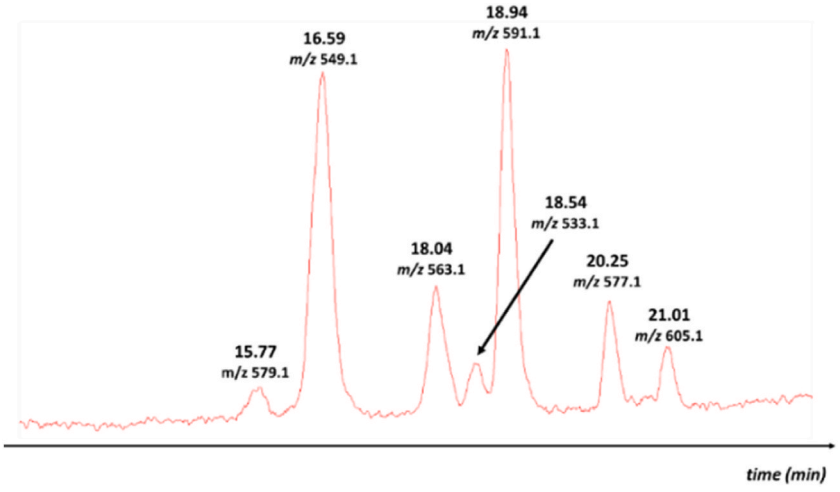

Fig. 1. LC-MS analysis (negative ionization mode) of the *Odontonema strictum* flavonoid ethanol extract: the Total Ion Current (TIC) chromatogram highlights the presence of 7 major signals. The *m/z* ratios correspond to the $[M - H]^-$ ions detected in the mass spectra.

Table 1
LC-MS/MS analysis (ESI negative ionization mode) of the *Odontonema strictum* flavonoid ethanol extract: overview of the MS data generated.

N°	Rt (min)	Composition $[M-H]^-$	Relative abundance (%)	*m/z* $[M-H]^-$	Δ(*m/z*) (ppm)	Fragment ions in LC-MS/MS	
						Aglycone ions	Sugar losses
1	16.6	$C_{25}H_{25}O_{14}$	38.7	549.1254	1.8	*m/z* 285	132 u/132 u
2	15.8	$C_{26}H_{27}O_{15}$	2.7	579.1360	1.7	*m/z* 285	162 u/132 u
3	18.0	$C_{26}H_{27}O_{14}$	8.8	563.1396	−0.9	*m/z* 285	146 u/132 u
4	18.9	$C_{27}H_{27}O_{15}$	8.4	591.1351	0.2	*m/z* 285	42 u, 18 u, 132 u, 132 u
5	16.5	$C_{26}H_{27}O_{13}$	9.3	547.1106	3.3	*m/z* 269	278 u[a]
6	18.4	$C_{25}H_{25}O_{13}$	4.1	533.1313	3.4	*m/z* 269	132 u/132 u
7	18.1	$C_{27}H_{29}O_{15}$	1.3	593.1462	−7.4	*m/z* 299	162 u/132 u
8	18.9	$C_{26}H_{27}O_{14}$	16.7	563.1396	−0.9	*m/z* 299	132 u/132 u
9	20.2	$C_{26}H_{27}O_{15}$	6.6	577.1528	−5.0	*m/z* 299	278 u[a]
10	21.0	$C_{28}H_{29}O_{15}$	3.4	605.1490	−2.6	*m/z* 299	42 u, 18 u, 132 u, 132 u

[a] the 278 u loss could correspond to a 132 u + 146 u but the intermediate ions are not detected.

reagent) the fractions containing the targeted flavonoid – R_f 0.47 (Fig. S2) were further subjected to repeated Sephadex LH-20 column chromatography to isolate the compound **1** (25 mg), as an amorphous powder with orange color. The isolated compound has been subjected to mass spectrometry analysis with a special attention paid at the accurate mass of the detected ions and at the fragment ions generated upon collision-induced dissociation experiments (CID). First of all, the deprotonated molecules, $[M-H]^-$ ions detected at *m/z* 549 correspond to the elemental composition $C_{25}H_{25}O_{14}$, as determined by high resolution mass spectrometry (Table 1).

These *m/z* 549 ions were further subjected to Collision-induced Dissociation (CID) experiments in the course of LC-MS/MS analysis to generate fragment ions for structural characterization. At low kinetic energy, 20 eV (Fig. 2A), the precursor ions mostly dissociate by generating two fragment ions that are observed at *m/z* 417 due to the loss of a 132 u pentose residue (xylose, apiose or ribose) and at *m/z* 285 due to the loss of two pentose residues that could be either consecutive (*m/z* 549 → *m/z* 417 → *m/z* 285) or unique (*m/z* 549 → *m/z* 285). Based on literature reports [21–23], the weaker intensity of the signal at *m/z* 417 compared to the *m/z* 285 signal indicates an *O*-diglycosyl structure. Increasing the collision energy up to 65 eV induces the production of aglycone fragment ions, as clearly observed in Fig. 2B. In particular, the presence of the $^{1,3}A^-$ fragment ions detected at *m/z* 151 points to luteolin or kaempferol aglycon, as featured in Fig. 3 [24,25]. However, the observation of the key-fragment ions at *m/z* 133, says $^{1,3}B^-$ ions, and 256 allows to propose a luteolin aglycone [25], as also confirmed by comparison with the CID spectrum of a standard luteolin.

The common glycosylation sites of flavone *O*-glycosides are at the 7-, 5- or 4'-*O* positions. Flavonoid 5-*O*-glycosides rarely meet and do not yield $[Y_0-H]^{-\cdot}$ fragment ions in negative ion mode [26]. The identification of glycosylation site can be performed on the basis of relative abundances of Y_0^- and $[Y_0-H]^{-\cdot}$ product ions. CID spectra obtained for deprotonated flavonoid **1** showed a radical aglycone ion ($[Y_0-H]^{-\cdot}$) at *m/z* 284 beside the Y_0^- ion at *m/z* 285, corresponding to the deprotonated luteolin. The radical aglycone ion ($[Y_0-H]^{-\cdot}$) is relatively more abundant ($[Y_0-H]^{-\cdot}/Y_0^- = 1.42$) than the deprotonated aglycone Y_0^- at high collision energy (65 eV) and favour 7-*O*-glycolsylation. In addition, the $^{1,3}B^-$ ions are pronounced for the flavonoid **1** and confirm the 7-*O*-glycosylation [27,28].

The ^1H and ^{13}C NMR spectra were recorded on the isolated flavonoid **1** dissolved in DMSO-d_6 and are all gathered in Figs. S3–12. The ^1H and ^{13}C NMR chemical shifts are reported in Table 2. The ^1H NMR spectrum features a total of six aromatic protons which resonate between δ_H 6.30 ppm and δ_H 7.45 ppm (Fig. S3). The three aromatic protons of the B-ring (Fig. 4) at δ_H 7.44 ppm (1H, dd, *J* =

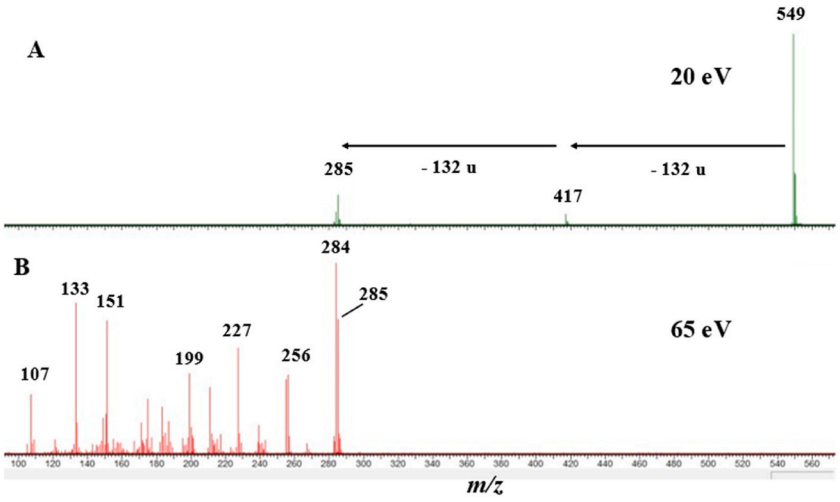

Fig. 2. LC-MS/MS analysis (negative ionization mode) of the *Odontonema strictum* flavonoid ethanol extract: CID spectra recorded at 20 eV and 65 eV (precursor ion kinetic energy) for the *m/z* 549 $[M-H]^-$ ions.

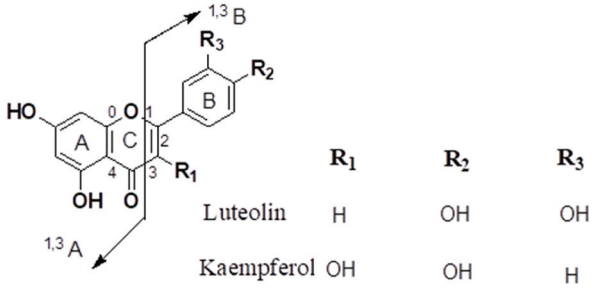

Fig. 3. CID of flavonoid aglycone ions: ^{1,3}A and ^{1,3}B refer to aglycone fragments containing A- and B-rings, respectively, and superscripts 1 and 3 indicate the broken C-ring bonds with charges retention on the A- or B-ring fragments [25].

2.22, 8.43 Hz, H-6'), 6.81 ppm (1H, d, $J = 8.43$ Hz, H-5') and 7.38 ppm (1H, d, $J = 2.22$ Hz, H-2') resonate in an ABX system, whereas the A-ring protons with δ_H 6.77 ppm (1H, d, $J = 2.16$ Hz, H-8) and 6.38 ppm (1H, d, $J = 2.16$ Hz, H-6) point to an AB system. The proton H-3 of the C-ring appears as a singlet at δ_H 6.69 ppm.

The HSQC spectrum showed in Fig. S8 allows determining the carbon atoms bearing these protons that are detected with δ_C 120.20 ppm (C-6'), 116.36 ppm (C-5'), 112.57 ppm (C-2'), 94.85 ppm (C-8), 99.61 ppm (C-6) and 102.44 ppm (C-3). The HMBC spectrum in Fig. S9 shows correlations from H-3 to δ_C 165.44 ppm (C-2), 182.10 ppm (C-4), 105.73 ppm (C-10) and 119.10 ppm (C-1'). The two aromatic protons of the A-ring (H-6 and H-8) correlate in HMBC with a carbon nucleus at δ_C 162.69 ppm (C-7). This value is an indication of glycosylation at that position. The downfield shifts observed for C-6 (δ_C 99.61 ppm) and C-8 (δ_C 94.85 ppm) confirm the glycosylation at C-7 of the aglycone. The other carbon nuclei of the aglycone which are quaternaries carbon atoms resonate at δ_C 161.47 ppm (C-5), 157.34 ppm (C-9), 146.88 ppm (C-3') and 153.40 ppm (C-4') as assigned by exploiting both the ^{13}C NMR spectrum (Fig. S6) and the DEPT 135 data (Fig. S7). The ^{1}H and ^{13}C NMR spectra data are also in good agreement with those previously reported in the literature [29,30].

The structure elucidation of the two pentose moieties is achieved using 1D and 2D NMR experiments. The well-resolved anomeric proton signals resonate at δ_H 5.17 ppm (1H, d, $J = 7.44$ Hz, H-1'') and 5.33 ppm (1H, d, $J = 1.44$ Hz, H-1‴) (Fig. S4). The analysis of the HMBC spectrum (Fig. S9) reveals a correlation between the anomeric proton at δ_H 5.17 ppm with the carbon at δ_C 162.69 ppm (C-7), which also confirms the glycosylation at that position of the aglycone. We deduce that the anomeric proton at δ_H 5.17 ppm belongs to the pentose residue directly attached to the aglycone and the one at δ_H 5.33 ppm belongs to the second pentose. The correlation spectrum HSQC (Fig. S8) allows identifying both anomeric carbons at δ_C 98.92 ppm (C-1'') and δ_C 109.33 ppm (C-1'''). Starting from the anomeric proton signals, 1D TOCSY, DQF-COSY and ^{1}H–^{1}H-COSY experiments (Figs. S10–15) allow the sequential assignments of the other protons of the pentoses, as previously described for other flavonoids glucosides [30,31]. Among these protons, four methine and three methylene groups are present and appear in the region δ_H 3.25−3.95 ppm, with characteristic splitting patterns (doublet,

Table 2
^{1}H and^{13}C NMR spectroscopic data for isolated compound **1** (600 MHz, δ_H, J in Hz).

Atome	^{1}H, δ (ppm); multiplicity (J in Hz)	^{13}C δ (ppm)
2	–	165.44
3	6.69; *s*	102.44
4	–	182.10
5	(-OH) 8.47; *s*	161.47
6	6.38; *d* (2.16)	99.61
7	–	162.69
8	6.77; *d* (2.16)	94.85
9	–	157.34
10	–	105.73
1'	–	119.10
2'	7.38; *d* (2.22)	112.57
3'	–	146.88
4'	–	153.40
5'	6.81; *d* (8.43)	116.36
6'	7.44; *dd* (8.43 and 2.22)	120.20
1''	5.17; *d* (7.44)	98.92
2''	3.53; *t* (7.8)	76.56
3''	3.43; brd	69.75
4''	3.75–3.78; brd	76.84
5''	3.30; *dd* (2.76)	64.35
1‴	5.33; *d* (1.44)	109.33
2‴	3.75–3.78; brd	76.43
3‴	–	79.63
4‴	3.89 (H_1); *d* (9.42) and 3.67 (H_2); *d* (9.42)	74.27
5‴	3.42; brd	65.98

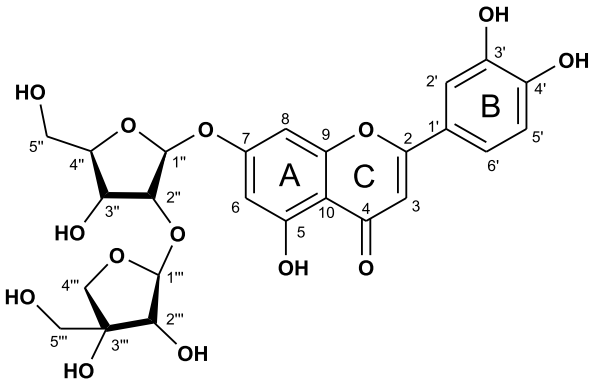

Fig. 4. Molecular structure of the isolated flavonoid **1** luteolin *7-O-[β*-D-apiofuranosyl-*(1 → 2)-O-β*-D-ribofuranoside].

triplet and broad). The pentose not directly linked to the aglycone possesses a quaternary carbon and a methylene group, as revealed by both ^{13}C and DEPT 135 NMR spectra. The methylene protons in position 4‴ (Fig. 4) are different and resonate at δ_H 3.89 ppm (1H, d, J = 9.42 Hz) and δ_H 3.67 ppm (1H, d, J = 9.42 Hz) in an AB system.

Based on all these MS and NMR data, the structure of flavonoid **1** is proposed to be luteolin 7-*O*-[β-D-apiofuranosyl-(1 → 2)-β-D-ribofuranoside], presented in Fig. 4. This flavone is identified for the first time as for us. Some isomers of the isolated molecule were previously isolated from *Sclerochiton vogelii* (Acanthaceae) [30] and *Justicia secunda* Vahl [31] and were respectively luteolin 7-*O*-[β-D-apiofuranosyl-(1 → 2)-β-D-xylopyranosyl] and luteolin 7-*O*-[β-apiofuranosyl-(1 → 2) β-xylopyranoside]. In these structures, the pentose directly linked to the aglycone is a xylose while in compound **1** it is a ribose. Spectroscopic characteristics in ^1H NMR of compound **1** are deepened, because the highest resolution used (600 MHz) allowed the assignation of all the aromatic protons and their coupling systems (AB and ABX). For example, the protons H-2' and H-6' resonate respectively as doublet and doublet of doublets respectively.

3.3. Other flavonoids characterization

The isolation of all the 10 flavonoids presented in Table 1 was not achieved, but we decided to gather as many as possible structural information mostly using LC-MS and LC-MS/MS experiments. The CID mass spectra of all detected flavonoid ions are presented in Figure S17.1-9 and the signature fragment ions are presented in Table 1. In particular, the monosaccharide losses leading to the aglycone ions are highlighted.

Compounds **2**, **3** and **6** with respective retention times at 15.8, 18.0 and 18.4 min (Table 1) are tentatively identified based on their MS/MS spectra analyses.

Compound **2** is detected as $[M-H]^-$ ions at *m/z* 579 that correspond to the molecular formula $C_{26}H_{27}O_{15}$, as measured using HRMS. The CID mass spectrum is presented in Figure S17.1 and the occurrence of fragment ions at *m/z* 417 suggests the loss of a hexose residue (typically a glucose), whereas the *m/z* 285 fragment ions arise from a consecutive 132 u loss, readily attributed to a pentose loss. The aglycone ions detected at *m/z* 285 are identified as luteolin ions, based on the data acquired for compound **1** and luteolin standard. The proposed structure is luteolin 7-*O*-[β-D-glycofuranosyl-(1 → 2)-*O*-β-D-ribofuranoside], as shown in Fig. 5. As far as compound **3** is concerned (Rt at 18 min and *m/z* 563), the HRMS data confirm the elemental composition presented in Table 1 and the CID mass spectrum is presented in Figure S17.2. Successive 146 u and 132 u losses, *m/z* 563 → *m/z* 417 → *m/z* 285, are again observed (see also Table 1) and suggest successive rhamnose and pentose losses. The fragmentation of the *m/z* 285 aglycone ions (higher collision energy regime) again confirms the presence of a luteolin. Compound **3** is tentatively identified as luteolin 7-*O*-[β-D-rhamnofuranosyl-(1 → 2)-*O*-β-D-ribofuranoside] (Fig. 5). As far as compound **6** (Rt 18.4 min) is concerned, beside the elemental composition that is readily confirmed upon HRMS experiments in Table 1, successive 132 u losses yielding the aglycone ions at *m/z* 269 (Figure S17.5). These aglycone ions were identified as apigenin ions by comparison with reference ions. Compound **6** is thus proposed to be apigenin 7-*O*-[β-D-apiofuranosyl-(1 → 2)-*O*-β-D-ribofuranoside] (Fig. 5).

As far as the other flavonoids are concerned, as shown in Table 1, all molecules possess a disaccharide, attached to the flavonoid aglycone at the common glycosylation site, say the 7-position [32]. The intersaccharide linkage could be rutinoside-like or neohesperidoside-like linkage, but the neohesperidoside linkage is probably present based on the NMR data for the isolated and full characterized flavonoid **1** and literature data [33]. All aglycones are flavones (luteolin or apigenin). Two specific cases have been detected and correspond to the *m/z* 591 (**4**) and 605 (**10**) ions.

4. Conclusions

In the present study, LC–MS and MS/MS analyses have revealed the wide array of flavonoids present in *Odontonema strictum* leaves. One flavone glycoside was isolated and fully characterized as luteolin 7-*O*-[β-D-apiofuranosyl-(1 → 2)-*O*-β-D-ribofuranoside], using tandem mass spectrometry and 1 D and 2 D NMR. Three other flavonoids glycosides with luteolin and apigenin aglycone were also

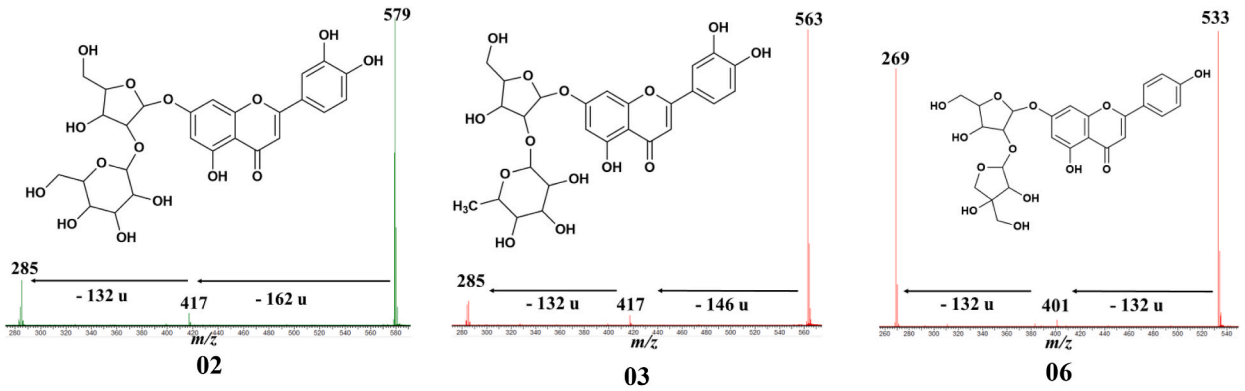

Fig. 5. Proposed molecular structure for compounds **2**, **3** and **6** detected at *m/z* 579, 563 and 533, respectively.

identified. Full description of the major flavonoids was done by the determination of the amount of each flavonoid present in the ethanol extract. The isolated flavonoid had the higher content with 38.68 %.

This study reveals the richness of *Odontonema strictum* in flavonoids and may justify its biological properties. This plant deserves to be valued because it is available and easy to grow.

Disclosure statement

The authors declare that there are no conflicts of interest.

Funding

This work was supported by the International Science Programme, ISP (UPPSALA UNIVERSITY, Sweden) through the project BUF:01. The bioprofiling platform supported by the European Regional Development Fund and the Wallonia Region (Belgium) is also acknowledged.

Data availability statement

All data are fully available without restriction.

CRediT authorship contribution statement

Jean Claude W. Ouédraogo: Writing – review & editing, Writing – original draft, Software, Methodology, Formal analysis, Data curation, Conceptualization. **Céline Henoumont:** Software, Formal analysis. **Irène Semay:** Software, Formal analysis. **Félix B. Kini:** Conceptualization. **Sophie Laurent:** Writing – review & editing, Validation. **Pascal Gerbaux:** Writing – review & editing, Validation, Supervision, Formal analysis. **Yvonne L. Bonzi – Coulibaly:** Writing – review & editing, Supervision, Funding acquisition.

Declaration of competing interest

The authors declare the following financial interests/personal relationships which may be considered as potential competing interests:Yvonne L Bonzi Coulibaly reports financial support was provided by International Science Programme (ISP).

Appendix A. Supplementary data

Supplementary data to this article can be found online at https://doi.org/10.1016/j.heliyon.2024.e37273.

References

[1] S. Ouédraogo, F. Kini, L. Serme, J.B. Nikiéma, A. Traoré, P.I. Guissou, M. Ndiaye, B. Bucher, R. Andriantsitohaina, Assessment of the hypotensive and vasodilator effects of extract and fractions from *Odontoneme strictum* (Acanthaceae), Ethnopharmacologia 36 (2005) 74–77.

[2] M. Nitiéma, M. Koala, L. Belemnaba, J.C.W. Ouédraogo, S. Ouédraogo, F.B. Kini, S. Ouédraogo, I.P. Guissou, Endothelium-independent vasorelaxant effects of anthocyanins-enriched extract from *Odontonema strictum* (Nees) Kuntze (Acanthaceae) flowers: Ca^{2+} channels involvement, Eur. J. Med. Plants 29 (2019) 1–11, https://doi.org/10.9734/ejmp/2019/v29i330155.

[3] L.P. Luhata, N.M. Munkombwe, P.M. Cheuka, H. Sikanyika, Phytochemical screening and *in vitro* antibacterial activity of *Odontonema strictum* (Acanthaceae) against selected bacteria, Int J Dev Res 5 (2015) 4655–4659.

[4] J.C.W. Ouédraogo, M. Koala, N. Ouédraogo, F.B. Kini, P. Gerbaux, Y.L. Bonzi-Coulibaly, Total phenolics and total flavonoid contents, antioxidant activity and flavonoids identification by high-performance liquid chromatography –tandem mass spectrometry of *Odontonema strictum* (Acanthaceae) leaves, Asian J. Plant Sci. Res. 7 (2017) 54–63.

[5] L.P. Luhata, N.M. Munkombwe, Isolation and characterisation of stigmasterol and β -sitosterol from *Odontonema strictum* (Acanthaceae), J Innovations Pharm Biol Sci. 2 (2015) 88–96.

[6] L.P. Luhata, T. Usuki, Antibacterial activity of β-sitosterol isolated from the leaves of *Odontonema strictum* (Acanthaceae), Bioorg Med Chem Lett. 48 (2021) 128248, https://doi.org/10.1016/j.bmcl.2021.128248.

[7] L.P. Luhata, T. Usuki, Free radical scavenging activities of verbascoside and isoverbascoside from the leaves of *Odontonema strictum* (Acanthaceae), Bioorg Med Chem Lett 59 (2022) 128528, https://doi.org/10.1016/j.bmcl.2022.128528.

[8] F.B. Kini, A. Saba, M. Tits, L. Angelot, P.I. Guissou, Analyse par Chromatographie et par Spectrométrie Electronique des Extraits de Feuilles de *Odontonema strictum* (Acanthaceae). Mise en Evidence de Flavonoïdes du type Flavone, J Soc Ouest-Afr Chim. 25 (2008) 117–121.

[9] L.P. Luhata, N.M. Munkombwe, H. Hatwiko, Isolation and ^{1}H-NMR identification of a tiliroside from *Odontonema strictum* (Acanthaceae), J. Pharmacogn. Phytochem. 5 (2016) 206–210.

[10] H. Mohamed, A. Hassane, O. Atta, Y. Song, Deep learning strategies for active secondary metabolites biosynthesis from fungi: harnessing artificial manipulation and application, Biocatal. Agric. Biotechnol. 38 (2021) 102195, https://doi.org/10.1016/j.bcab.2021.102195.

[11] H. Slika, H. Mansour, N. Wehbe, S.A. Nasser, R. Iratni, G. Nasrallah, A. Shaito, T. Ghaddar, F. Kobeissy, A.H. Eid, Therapeutic potential of flavonoids in cancer: ROS-mediated mechanisms, Biomed. Pharmacother. 146 (2022) 112442, https://doi.org/10.1016/j.biopha.2021.112442.

[12] M. Khalid, S. Rahman, M. Bilal, D.F. Huang, Role of flavonoids in plant interactions with the environment and against human pathogens - a review, J. Integr. Agric. 18 (2019) 211–230, https://doi.org/10.1016/S2095-3119(19)62555-4.

[13] O. Ilboudo, S. Bonzi, I. Tapsoba, I. Somda, Y.L. Bonzi-Coulibaly, *In vitro* antifungal activity of flavonoid diglycosides of *Mentha piperita* and their oxime derivatives against two cereals fungi, C R Chim 19 (2016) 857–862, https://doi.org/10.1016/j.crci.2015.11.023.

[14] A. Sankara, J.C.W. Ouédraogo, L. Pignolet, M.F. Thévenon, Y.L. Bonzi-Coulibaly, Chemical profiles and anti-termite activity of hydrodistillation residues from three aromatic plants acclimated in Burkina Faso, J. Agric. Sci. 12 (2020) 245–256, https://doi.org/10.5539/jas.v12n8p245.

[15] K. Bairwa, I.N. Singh, S.K. Roy, J. Grover, A. Srivastava, S.M. Jachak, Rotenoids from *Boerhaavia diffusa* as potential anti-inflammatory agents, J Nat Prod 76 (2013) 1393–1398, https://doi.org/10.1021/np300899w.

[16] B. Bhattarai, S.K. Steffensen, D. Staerk, B.B. Laursen, I.S. Fomsgaard, Data-dependent acquisition-mass spectrometry guided isolation of new benzoxazinoids from the roots of Acanthus mollis L, Int. J. Mass Spectrom. 474 (2022) 116815, https://doi.org/10.1016/j.ijms.2022.116815.

[17] C. Decroo, E. Colson, M. Demeyer, V. Lemaur, G. Caulier, I. Eeckhaut, J. Cornil, P. Flammang, P. Gerbaux, Tackling saponin diversity in marine animals by mass spectrometry: data acquisition and integration, Anal. Bioanal. Chem. 409 (12) (2017) 3115–3126, https://doi.org/10.1007/s00216-017-0252-7.

[18] E. Colson, P. Savarino, E.J.S. Claereboudt, G. Cabrera-Barjas, M. Deleu, L. Lins, I. Eeckhaut, P. Flammang, P. Gerbaux, Enhancing the membranolytic activity of *Chenopodium quinoa* saponins by fast microwave hydrolysis, Molecules 25 (1731) (2020) 1–20, https://doi.org/10.3390/molecules25071731.

[19] A. Palma, M.J. Díaz, M. Ruiz-Montoya, E. Morales, I. Giraldez, Ultrasound extraction optimization for bioactive molecules from *Eucalyptus globulus* leaves through antioxidant activity, Ultrason. Sonochem. 76 (2021) 105654, https://doi.org/10.1016/j.ultsonch.2021.105654.

[20] K.H. Pilepić, Z. Yang, J. Chen, X. Chen, Y. Wang, J. Zhao, S. Mihaljević, S.P. Li, Flavonoids in natural and tissue cultured materials of Epimedium alpinum identified by using UHPLC-Q-TOF-MS/MS, Int. J. Mass Spectrom. 434 (2018) 222–232, https://doi.org/10.1016/j.ijms.2018.09.026.

[21] K. Ablajan, Z. Abliz, X.Y. Shang, J.M. He, R.P. Zhang, J.G. Shi, Structural characterization of flavonol 3,7-di-*O*-glycosides and determination of the glycosylation position by using negative ion electrospray ionization tandem mass spectrometry, J. Mass Spectrom. 41 (2006) 352–360, https://doi.org/10.1002/jms.99.

[22] M. Beszterda, R. Franski, Elucidation of glycosylation sites of kaempferol di-*O*-glycosides from methanolic extract of the leaves of *Prunus domestica* subsp, Syriaca. Rapid Commun Mass Spectrom 35 (2021) e9100, https://doi.org/10.1002/rcm.9100.

[23] F. Ferreres, R. Llorach, A. Gil-Izquierdo, Characterization of the interglycosidic linkage in di-, tri-, tetra- and pentaglycosylated flavonoids and differentiation of positional isomers by liquid chromatography/electrospray ionization tandem mass spectrometry, J. Mass Spectrom. 39 (2004) 312–321, https://doi.org/10.1002/jms.586.

[24] F. Cuyckens, Y.L. Ma, G. Pocsfalvi, M. Claeys, Tandem mass spectral strategies for the structural characterization of flavonoid glycosides, Analusis 28 (10) (2000) 888–895, https://doi.org/10.1051/analusis:2000280888.

[25] M. Sliwka-Kaszynska, I. Anusiewicz, P. Skurski, The mechanism of a retro-diels–alder fragmentation of luteolin: theoretical studies supported by electrospray ionization tandem mass spectrometry results, Molecules 27 (1032) (2022) 1–16, https://doi.org/10.3390/molecules27031032.

[26] M. Beszterda, R. Franski, Electrospray ionisation mass spectrometric behaviour of flavonoid 5-*O*-glucosides and their positional isomers detected in the extracts from the bark of *Prunus cerasus* L. and *Prunus avium* L, Phytochem. Anal. (2020) 1–7, https://doi.org/10.1002/pca.2991.

[27] F. Cuyckens, M. Claeys, Determination of the glycosylation site in flavonoid mono-*O*-glycosides by collision-induced dissociation of electrospray-generated deprotonated and sodiated molecules, J. Mass Spectrom. 40 (2005) 364–372, https://doi.org/10.1002/jms.794.

[28] E. Hvattum, D. Ekeberg, Study of the collision-induced radical cleavage of flavonoid glycosides using negative electrospray ionization tandem quadrupole mass spectrometry, J. Mass Spectrom. 38 (2003) 43–49, https://doi.org/10.1002/jms.398.

[29] L. Ge, J. Li, H. Wan, K. Zhang, W. Wu, X. Zou, S. Wu, B. Zhou, J. Tian, X. Zeng, Novel flavonoids from *Lonicera japonica* flower buds and validation of their anti-hepatoma and hepatoprotective activity in vitro studies, Ind. Crops Prod. 125 (2018) 114–122, https://doi.org/10.1016/j.indcrop.2018.08.073.

[30] M. Lamidi, M.L. Rondi, R. Faure, L. Debrauwer, L. Nze-Ekekang, G. Balansard, E. Ollivier, Flavonoid glycosides from *Sclerochiton vogelii*, C R Chim 9 (2006) 1309–1313, https://doi.org/10.1016/j.crci.2006.05.004.

[31] E.N. Koffi, C. Le Guernevéc, P.R. Lozano, E. Meudec, F.A. Adjé, Y.A. Bekro, Y.F. Lozano, Polyphenol extraction and characterization of *Justicia secunda* Vahl leaves for traditional medicinal uses, Ind. Crops Prod. 49 (2013) 682–689, https://doi.org/10.1016/j.indcrop.2013.06.001.

[32] F. Cuyckens, M. Claeys, Mass spectrometry in the structural analysis of flavonoids, J. Mass Spectrom. 39 (2004) 1–15, https://doi.org/10.1002/jms.585.

[33] M. Satterfield, J.S. Brodbelt, Structural characterization of flavonoid glycosides by collisionally activated dissociation of metal complexes, J. Am. Soc. Mass Spectrom. 12 (2001) 537–549, https://doi.org/10.1016/S1044-0305(01)00236-7.